JOC The Journal of Organic Chemistry

Article

pubs.acs.org/joc

Rational Design, Synthesis, and Characterization of Deep Blue Phosphorescent Ir(III) Complexes Containing (4′-Substituted-2′-pyridyl)-1,2,4-triazole Ancillary Ligands

Hea Jung Park,[†] Ji Na Kim,[†] Hyun-Ji Yoo,[†] Kyung-Ryang Wee,[‡] Sang Ook Kang,[‡] Dae Won Cho,[‡] and Ung Chan Yoon*[,†]

[†]Department of Chemistry, Pusan National University, Busan 609-735, Korea

[‡]Department of Advanced Materials Chemistry, Korea University, 2511 Sejong-ro, Sejong 339-700, Korea

Supporting Information

ABSTRACT: On the basis of the results of frontier orbital considerations, 4-substituted-2′-pyridyltriazoles were designed to serve as ancillary ligands in 2-phenylpyridine main ligand containing heteroleptic iridium(III) complexes that display deep blue phosphorescence emission. The iridium(III) complexes, **Ir1**−**Ir7**, prepared using the new ancillary ligands, were found to display structured, highly quantum efficient (Φ_p = 0.20−0.42) phosphorescence with emission maxima in the blue to deep blue 448−456 nm at room temperature. In accord with predictions based on frontier orbital considerations, the complexes were observed to have emission properties that are dependent on the electronic nature of substituents at the C-4 position of the pyridine moiety of the ancillary ligand. Importantly, placement of an electron-donating methyl group at C-4′ of the pyridine ring of the 5-(pyridine-2′-yl)-3-trifluoromethyl-1,2,4-triazole ancillary ligand leads to an iridium(III) complex that displays a deep blue phosphorescence emission maximum at 448 nm in both the liquid and film states at room temperature. Finally, an OLED device, constructed using an Ir-complex containing the optimized ancillary ligand as the dopant, was found to emit deep blue color with a CIE of 0.15, 0.18, which is close to the perfect goal of 0.15, 0.15.

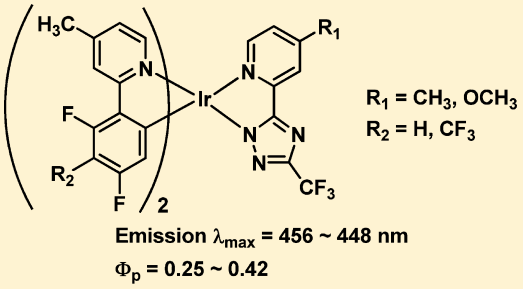

INTRODUCTION

Because of numerous advantageous features including a good viewing angle, lower power consumption and high-quality image processing, organic light-emitting diode (OLED) based systems are becoming next-generation display devices and solid state light sources. In the light producing process of an OLED system, an electron and a hole injected into the respective LUMO and the HOMO of the organic electroluminescent layer combine to form an exciton, which relaxes to its ground state with emission of light. The color of the emitted light, typically in the visible region ranging from red to blue, is determined by the energy of the band gap between LUMO and HOMO of the electroluminescent layer. Radiation emitted from OLEDs may arise theoretically through either fluorescence from singlet excited states or phosphorescence from triplet excited states of light emitter organic molecules in the electroluminescent layer. Since no electron-spin control mechanism operates during electrical excitation and decay in OLEDs, electron and hole injection and recombination occur randomly to generate approximately one singlet exciton with an antisymmetric spin for every three triplet excitons with a symmetric spin configuration. Because molecular ground states are typically spin-antisymmetric singlets, relaxation of singlet excitons conserves spin and efficiently generates fluorescence emission, while triplet excitons need to undergo spin inversion through a spin orbit coupling process, and as a result, they do not normally effectively emit light to form the singlet ground state.

Because of these phenomena, the energy residing in triplet excitons is not typically used for efficient light emission in OLEDs, and consequently, it is wasted. Thus, in an OLED, where a fluorescent material is employed as or doped into the electroluminescent layer, the maximum internal quantum yield for light emission is ca. 25%. However, if the efficiency of spin−orbit coupling in triplet excitons can be enhanced by taking advantage of the heavy atom phenomenon, the efficiency of intersystem crossing between triplet excited and singlet ground state can be greatly increased. In this case, triplet excitons will more efficiently relax to singlet ground states by phosphorescence emission. Thus, in an optimized OLED, all triplet excitons are utilized for light emission, and as a result, all of the electrogenerated singlet and triplet excitons undergo light emission to yield a theoretically maximum internal efficiency of 100%.[1,2]

Materials that phosphoresce highly efficiently are typically incorporated in electroluminescent layers of OLEDs to transform triplet excitons into light. Because the spin−orbit coupling enhancement by heavy atoms is proportional to the fourth

Received: June 20, 2013
Published: July 18, 2013

ACS Publications © 2013 American Chemical Society

dx.doi.org/10.1021/jo4012514 | J. Org. Chem. 2013, 78, 8054−8064

power of the atomic number of the atom, complexes of heavy atoms such as platinum (Pt), iridium (Ir), europium (Eu), and terbium (Tb) have been utilized to promote the efficiency of intersystem crossing and phosphorescence emission.[2−5] Iridium complexes have been shown to be very effective in this regard because they are highly phosphorescent at room temperature and have short triplet lifetimes.[6] However, thus far the development of the phosphorescent OLEDs, which have excellent emission quantum yields and ideal color coordinates and lifetimes, is still at an early stage. Studies in this area have recently resulted in the development of a blue light-emitting phosphorescent iridium complex called FIrpic (iridium(III) bis[2-(2′,4′-difluorophenyl)-pyridinato-*N*,$C^{2'}$]picolinate)[7] and a red light-emitting phosphorescent material called Ir(btp)$_2$(acac) (iridium(III) bis[2-(2′-benzothienyl)pyridinato-*N*,$C^{2'}$](acetylacetonate)).[3] However, much work remains to be done to improve the color purity, efficiency, solubility and lifetime of iridium complexes used for OLEDs.

As mentioned above, the color of light emitted by OLEDs is determined by the energy of the band gap between the LUMO and HOMO of the electroluminescent layer. An evaluation of the electronic characteristics of the iridium(III) complex, tris-2-phenylpyridinato-*N*,C^2, Ir(ppy)$_3$, (TPPI) shows that its LUMO is largely localized on the pyridine ring of the main ligand 2-phenylpyridine while its HOMO is mainly localized on the phenyl ring of the main ligand.[8] As a consequence of these properties, electron-donating groups on the pyridyl group of the main ligand, especially at C-4, lead to an increase in the energy of the LUMO while the presence of electron-withdrawing groups on the phenyl ring of this ligand lowers the energy of the HOMO. Thus, a strategy involving the positionally selective introduction of substituents with different electronic characters should be useful to control the energy of the band gap and, thus, the wavelength of emission of electroemissive substances.

Yamashita and his co-workers have shown[9] that introduction of both an electron-withdrawing trifluoromethyl (CF_3) group at C-3 and fluoro groups at C-2 and C-4 on the phenyl ring of the phenylpyridinato-*N*,C^2 main ligand coupled with introduction of an electron-donating methyl group at C-4 of the pyridine ring of the main ligand gives rise to an iridium complex that displays an extreme blue shift in the phosphorescent emission compared to TPPI at room temperature. Furthermore, using this substitution pattern in combination with replacement of one of three of 2-phenylpyridine main ligand by an ancillary 5-(2′-pyridyl)-3-trifluoromethyl-1,2,4-triazole, Yamashita devised a blue phosphorescent iridium complex whose emission maximum is remarkably shorter (see below) than that of the well-known blue emissive iridium bis(4,6-difluorophenyl-pyridinato)-picolinate (FIrpic).

Recently we initiated investigations aimed at developing new, blue phosphorescent iridium(III) complexes. The strategy employed to design substances that have optimal emission characteristics focused on structures that contain properly substituted 2-phenylpyridine main ligands and a variety of substituted picolinate and pyridyltriazole ancillary ligands incorporated into heteroleptic octahedral Ir(III) complexes. The goal of the effort was to determine if substitution patterns in the main and ancillary ligands could be uncovered that enable the complexes to emit light efficiently in a deeper blue wavelength region than do FIrpic or the complex developed by Yamashita. Guided by expectations arising from considerations of substituent effects on the energies of HOMOs and LUMOs, we designed several Ir(III) complexes containing substituted phenylpyridinato-*N*,C^2 main and 5-(2′-pyridyl)-3-trifluoromethyl-1,2,4-triazole ancillary ligands. These complexes contain properly positioned electron-donating substituents at the C-4 of the pyridyl moiety of the ancillary ligand and electron-donating substituents at C-4 of the pyridine ring and electron-withdrawing groups at C-2, -3, and -4 of the phenyl ring of the phenylpyridine main ligand. In the studies described below, we prepared and characterized these rationally designed Ir(III) complexes (**Ir1**−**Ir7**, Figure 1)

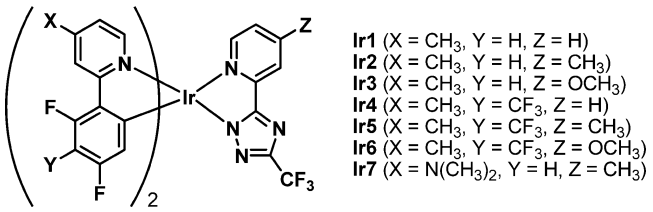

Figure 1. Structures of blue phosphorescent iridium(III) complexes **Ir1**−**Ir7** containing substituted phenylpyridine main and pyridyltriazole ancillary ligands.

and evaluated their photophysical properties. The results arising from this effort demonstrate that the iridium complex containing 5-(4′-methylpyridine-2′-yl)-3-trifluorormethyl-1,2,4-triazolate ancillary ligand, as predicted, displays deeper blue phosphorescence in its solution and film states at room temperature than currently known complexes and that this optimal complex can be used in the electroluminescent layer emission of an OLED that emits deeply blue light that has color coordinates near to the ideal value.

RESULTS AND DISCUSSION

Synthesis and Characterization of Designed Heteroleptic Iridium(III) Complexes. As stated above, an important strategy for the design for blue phosphorescent iridium(III) complexes that contain phenylpyridine main and variously structured ancillary ligands focuses on control of the HOMO−LUMO energy gap by properly positioned substituents.[10] Using this approach we have designed and prepared the Ir(III) complexes **Ir1**−**Ir7**, which contain substituted 2-phenylpyridine main ligands and 5-(4′-substituted-pyridine-2′-yl)-3-trifluorormethyl-1,2,4-triazolate ancillary ligands. The 2-phenylpyridine derivatives, **16**, **17**, and **19**, serving as the main ligands of the iridium complexes, were prepared by using a slight modification of the previously described method employing palladium-catalyzed coupling of aryl-boronates with 2-bromopyridines (Scheme 1).[9,11] Preparation of the pyridyltriazole ancillary ligands **9**, **10**, and **12**, required for formation of these complexes, utilized [2 + 3] cycloaddition reactions of appropriately substituted 2-pyridylnitriles **5** and **6** with trifluoroacetic acid hydrazide **8** (Scheme 1).[12] Finally, a two-step route (Scheme 2) was utilized for preparation of the heteroleptic iridium complexes **Ir1**−**Ir7**.[13] In the sequence, $IrCl_3 \cdot 3H_2O$ is reacted with an excess of the desired 2-phenylpyridine main ligand to give a μ-chlorobridged dimer, which is then converted to the corresponding heteroleptic complex by substitution of the bridging chlorides with the appropriate bidentate, monoanionic 4-substituted-pyridyl triazole ancillary ligand. By using this procedure, the iridium complexes are produced as pure substances in 30−51% yields. The single exception is **Ir6**, which in our hands could not be purified completely.

dx.doi.org/10.1021/jo4012514 | J. Org. Chem. 2013, 78, 8054−8064

Scheme 1. Synthesis of Ancillary (9, 10, and 12) and Main (16, 17, and 19) Ligands

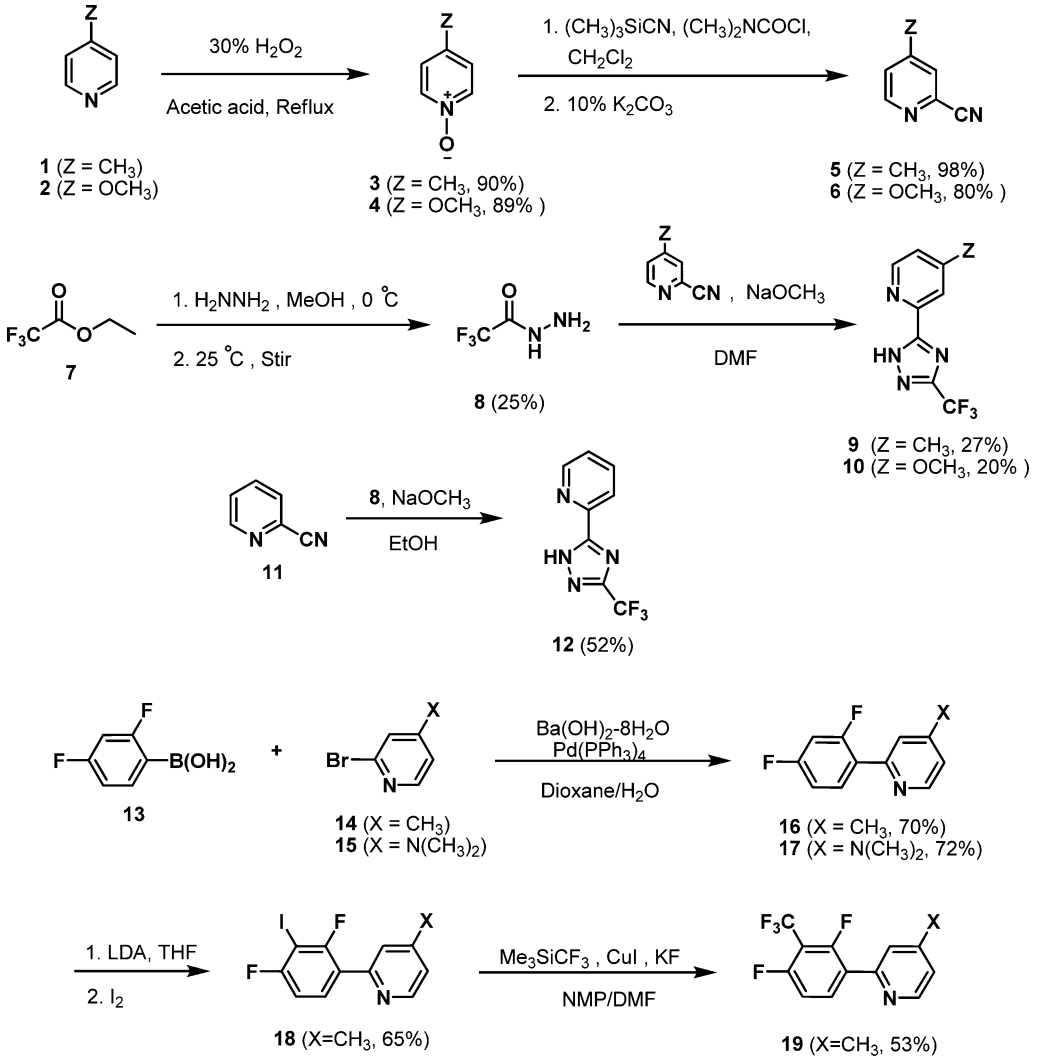

Scheme 2. Synthesis of μ-Chlorobridged Dimer Complexes 20−22 and Iridium(III) Complexes Ir1−Ir7

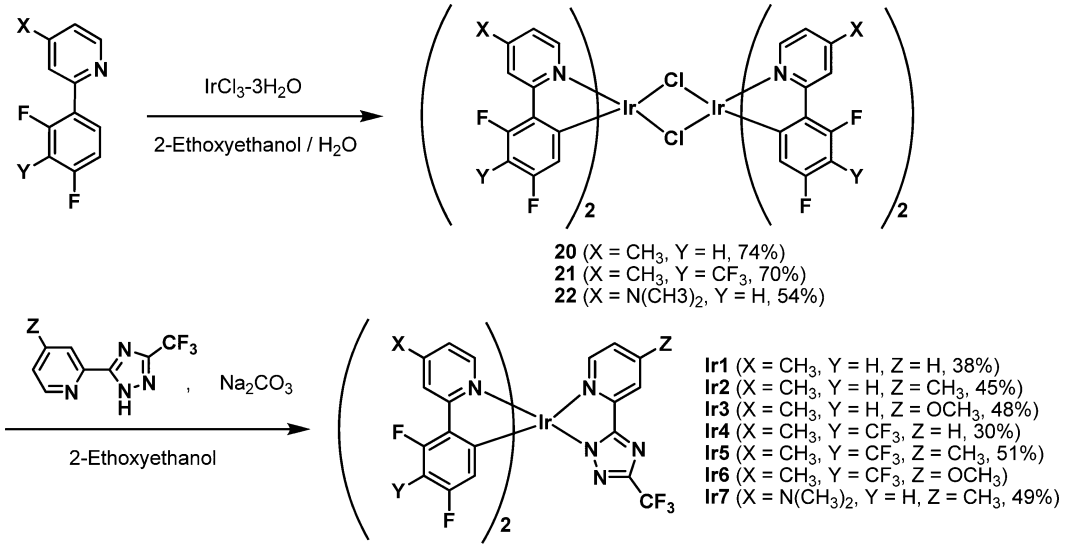

The synthesized iridium complexes were fully characterized by using NMR spectroscopy and mass spectrometry. In addition, X-ray crystallographic structure determinations were carried out on **Ir2**, **Ir3** and **Ir5**. (Figure 2, Table 1). The X-ray diffraction results show that, as expected, iridium in the complexes is octahedrally coordinated by the two main (2-phenylpyridine)

dx.doi.org/10.1021/jo4012514 | J. Org. Chem. 2013, 78, 8054−8064

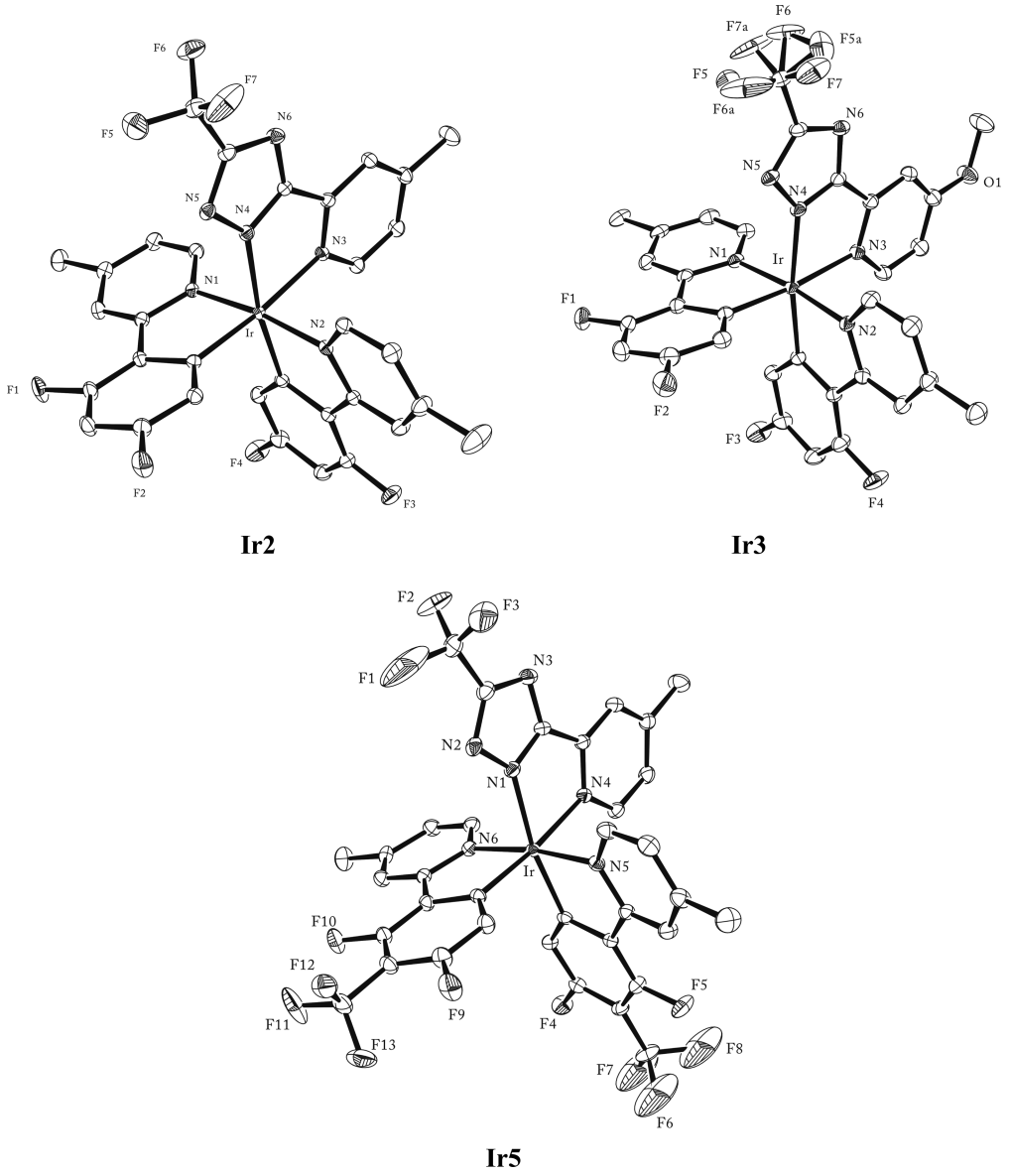

Figure 2. ORTEP plots of X-ray data for iridium complexes **Ir2**, **Ir3**, and **Ir5**. Hydrogen atoms and solvent molecules are omitted for clarity.

and one ancillary (pyridyltriazole) ligands and that the complexes have meridional configurations and consist of racemic mixtures. In addition, the data collected for **Ir1** and **Ir4** matched those previously reported for these substances by Yamashita and co-workers.[9]

Photophysical and Electrochemical Properties of Ir1−Ir7. In Figure 3 are displayed absorption and phosphorescence spectra of the synthesized iridium complexes **Ir1**−**Ir7**. Important photophysical data for these substances are listed in Table 2. In solution states, **Ir1**−**Ir7** display weak absorption bands in the 416−426 nm region. The new iridium complexes display strong and structured phosphorescence with emission maxima in the deep blue or blue 448−456 nm region and with high emission quantum efficiencies (Φ_p) between 0.20 and 0.42 at room temperature (Table 1). In addition, the emission spectra of the complexes in the film states are similar to those for the solution states, showing that a significant bathochromic shift does not take place as a result of $\pi-\pi$ stacking in the latter state. For comparison purposes, emission spectra of **Ir1**−**Ir3** and **Ir5** are given in Figure 4. Inspection of the spectra shows that electron-donating methyl or methoxy substitution at C-4′ of the 5-(pyridine-2′-yl)-3-trifluoromethyl-1,2,4-triazole ancillary ligand has a significant impact on the spectroscopic properties of the heteroleptic iridium complexes. These substituents promote modestly large (8 nm) hypsochromic shifts of the phosphorescence emission maximum. Particularly interesting is the fact that complex **Ir5** (emission λ_{max} = 448 nm) displays more deeply blue phosphorescence than that of the previously reported[9] **Ir4** (λ_{max} = 448 nm reported earlier[9] and λ_{max} = 456 nm measured in our laboratory). In addition, **Ir2**, which does not contain an electron-withdrawing trifluoromethyl substituent on the main ligand, has a phosphorescence maximum 456 nm, which is similar to that of **Ir4**. Moreover, the presence of the strong electron-donating *N*,*N*-dimethylamine group at C-4 of the pyridine main ligand in complex **Ir7** causes a significant 13 nm bathochromic shift of the emission maximum in solution at room temperature. Interestingly, in the film state this complex displays an emission maximum that is 20 nm blue-shifted compared to that of the substance in the solution state (Figure 5). Measured phosphorescence lifetimes (τ) of **Ir2**, **Ir3** and **Ir5** at

dx.doi.org/10.1021/jo4012514 | J. Org. Chem. 2013, 78, 8054−8064

Table 1. Crystallographic Data and Structure Refinements of Ir2, Ir3, and Ir5

identification code	Ir2	Ir3	Ir5
empirical formula	$C_{34}H_{24}Cl_2F_7IrN_6$	$C_{35}H_{24}Cl_6F_7IrN_6O$	$C_{36}H_{22}Cl_2F_{13}IrN_6$
formula weight	912.69	1082.50	1048.70
temperature	174(2) K	173(2) K	293(2) K
wavelength	0.71073 Å	0.71073 Å	0.71073 Å
crystal system	monoclinic	triclinic	triclinic
space group	$P2(1)/n$	$P\bar{1}$	$P\bar{1}$
unit cell dimensions			
a (Å)	11.2827(11) Å	10.65690(10) Å	10.3490(2) Å
b (Å)	19.8394(19) Å	17.5703(2) Å	11.8478(2) Å
c (Å)	14.7376(14) Å	22.4981(4) Å	15.8534(2) Å
α (deg)	90°	107.3280(10)°	109.2570(10)°
β (deg)	90.385(3)°	94.5960(10)°	91.9040(10)°
γ (deg)	90°	102.6350(10)°	97.1330(10)°
volume	3298.8(5) Å^3	3876.06(9) Å^3	1815.15(5) Å^3
Z	4	4	2
density (calculated)	1.838 Mg/m^3	1.855 Mg/m^3	1.919 Mg/m^3
absorption coefficient	4.285 mm^{-1}	3.931 mm^{-1}	3.930 mm^{-1}
$F(000)$	1776	2104	1016
crystal size	0.29 × 0.15 × 0.12 mm^3	0.52 × 0.34 × 0.29 mm^3	0.12 × 0.11 × 0.09 mm^3
theta range for data collection	1.72−26.00°	0.96−28.35°	1.36−28.44°
index ranges	$-13 \le h \le 13$	$-14 \le h \le 14$	$-13 \le h \le 13$
	$-24 \le k \le 24$	$-23 \le k \le 23$	$-15 \le k \le 15$
	$-18 \le l \le 16$	$-30 \le l \le 29$	$-21 \le l \le 21$
reflections collected	28979	69348	32416
independent reflections	6480 [R(int) = 0.0298]	19098 [R(int) = 0.0319]	9010 [R(int) = 0.0312]
completeness to theta	26.00° 100.0%	28.35° 98.6%	28.44° 98.6%
absorption correction	semiempirical from equivalents	semiempirical from equivalents	semiempirical from equivalents
max and min transmission	0.6251 and 0.3706	0.3952 and 0.2343	0.7187 and 0.6499
refinement method	full-matrix least-squares on F^2	full-matrix least-squares on F^2	full-matrix least-squares on F^2
data/restraints/parameters	6480/0/461	19098/0/1037	9010/3/509
goodness-of-fit on F^2	1.026	1.032	1.054
final R indices [$I > 2\sigma(I)$]	$R1$ = 0.0199, $wR2$ = 0.0509	$R1$ = 0.0367, $wR2$ = 0.0901	$R1$ = 0.0451, $wR2$ = 0.1246
R indices (all data)	$R1$ = 0.0215, $wR2$ = 0.0517	$R1$ = 0.0489, $wR2$ = 0.0969	$R1$ = 0.0501, $wR2$ = 0.1289
largest diff. peak and hole	1.024 and −0.556 e Å^{-3}	2.071 and −1.720 e Å^{-3}	5.147 and −2.667 e Å^{-3}

77 K were 3.15, 3.57, and 3.58 μs, respectively, which are in the similar ranges with previously reported work on a family of iridium(III) complexes.[14]

The respective HOMO and LUMO energies of complexes **Ir1**−**Ir7**, experimentally determined by using oxidation potential (Figure 6) and band gap data, were found to be in the ranges of −5.48 to −5.84 eV (vs ferrocene −4.8 eV) and −2.76 to −3.06 eV, respectively (Table 3 and Figure 7). The results show that **Ir2** and **Ir3** have larger HOMO−LUMO band gap energies than does **Ir1**. Thus, paralleling the results of phosphorescence measurements, electron-donating group substitution at C-4 of the pyridine ring of ancillary ligand leads to lower HOMO energies and corresponding higher LUMO energies. Interestingly, **Ir2** and **Ir3** possess similar HOMO and LUMO energies to **Ir4**, which has an electron-withdrawing trifluoromethyl group at C-3 of the phenyl ring of the main ligand and is missing an electron-donating methyl group on the ancillary ligand. Moreover, **Ir5** has the lowest HOMO energy and the largest HOMO−LUMO band gap energy among all of the synthesized iridium complexes. This property results from the introduction of an electron-withdrawing trifluoromethyl group on the main ligand and an electron-donating methyl group on the ancillary ligand. Finally, **Ir7**, which contains a strongly electron-donating *N*,*N*-dimethylamine group at C-4 of the pyridine ring of main ligand, has HOMO and LUMO energies of −5.48 and −2.76 eV, respectively.

OLED Device Constructed Using Iridium Complex Ir5. The use of **Ir5**, the Ir(III) complex observed to display optimal blue emission (λ_{max} = 448 nm), as a dopant emitter in the emissive layer of a simple OLED device was explored. The device configuration employed is ITO/NPB (500 nm)/TAPC (350 nm)/CDBP (100 nm)/CDBP:Ir6 (10%) (500 nm)/$Me_2Si(TAZ)_2$ (600 nm)/LiF:Al (Figure 8). In Figure 9 are displayed I−V−L curves and current efficiencies of the device in comparison to one constructed employing **FIr6** as the dopant emitter (structure given in Figure 9). As can be seen by viewing the results, the OLED device made with **Ir5** emits deep blue light corresponding to CIE (0.15, 0.18), which is very near the perfect goal of (0.15, 0.15), although the emission efficiency of **Ir5** based OLED device is lower under the OLED configuration comparing **Fir6**.

■ CONCLUSIONS

In the effort described above, we have utilized a strategy that is derived from frontier orbital considerations to design blue phosphorescent iridium(III) complexes. To explore the predicted effects of electron-donating and -withdrawing group substituents on the emission properties of these complexes containing a (4′-susbstituted pyridine-2′-yl)-1,2,4-triazole ancillary ligand,

dx.doi.org/10.1021/jo4012514 | J. Org. Chem. 2013, 78, 8054−8064

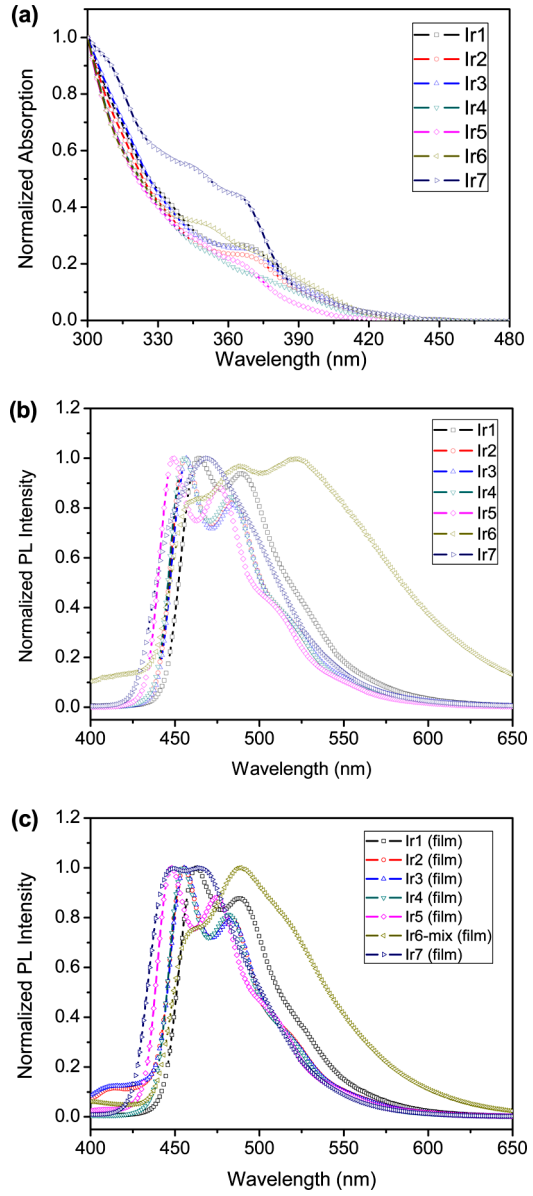

Figure 3. (a) UV−vis absorption spectra, (b) phosphorescence spectra in solution, and (c) the film states of **Ir1**−**Ir7**.

complexes **Ir1**−**Ir7** were synthesized and structurally characterized. The emission maxima of the synthesized iridium(III) complexes are in the blue 448−464 nm region, and these substances have high emission quantum efficiencies of 0.20−0.42 at room temperature. The results of photophysical studies with these complexes show that introduction of an electron-donating methyl or methoxy group at C-4 of the pyridine ring of the ancillary ligand leads to an increase in the energy of the HOMO−LUMO band gap and leads to a hypsochromic shift of phosphorescence emission. In an addition, as noted previously, introduction of an electron-withdrawing trifluoromethyl group at C-3 of the phenyl ring of the main ligand also greatly lowers the emission wavelength by 8 nm. The emission maximum of **Ir4** (456 nm) and **Ir5** (448 nm) are 8 nm lower than those of **Ir1** (464 nm) and **Ir2** (456 nm), respectively. These findings demonstrate that **Ir5** has an emission maximum that is 8 nm shorter than that of the complex **Ir4**, previously described by Yamashita and investigated thoroughly in this effort.[9] In addition to providing a potentially useful blue emitting substance for OLED studies, the current investigation has validated a strategy for the design of color selective emissive materials that is based on a consideration of substituent effects on the differences in energies of frontier (HOMO and LUMO) orbitals.

EXPERIMENTAL SECTION

Chemicals and Instruments. All reagents were obtained from commercial sources and used without further purification, and solvents were dried by using standard procedures.

^{1}H (300 MHz) and ^{13}C NMR (75 MHz) spectra were recorded on $CDCl_3$ and CD_3OD as solvents, and chemical shifts are reported in parts per million relative to $CHCl_3$ (7.26 ppm for ^{1}H NMR and 77.0 ppm for ^{13}C NMR) and CH_3OH (3.31 ppm for ^{1}H NMR and 49.0 ppm for ^{13}C NMR) as internal standards. High resolution (HRMS) mass spectra were obtained by use of quadrupole mass analyzer, electron impact ionization unless otherwise noted.

4-Methylpyridine *N*-oxide (3). This substance was prepared by using the method of Taylor and Crovetti.[15] To a solution of 4-methylpyridine (**1**, 3.0 mL, 30 mmol) in glacial acetic acid (20 mL) was added 30% hydrogen peroxide (2.9 mL, 30 mmol). The reaction mixture was stirred at reflux for 24 h and concentrated in vacuo to produce **3** (3.0 g, 27 mmol, 90%) as a bright yellow solid, which was used without further purification or characterization.[16]

4-Methoxypyridine *N*-oxide (4). To a solution of 4-methoxylpyridine (**2**, 10.0 mL, 85.9 mmol) in glacial acetic acid (50 mL) was added 30% hydrogen peroxide (8.4 mL, 85.9 mmol). The mixture was stirred at reflux for 24 h and concentrated in vacuo giving **4** (9.6 g, 76.5 mmol, 89%) as an oil, which was used without further purification or characterization.[16]

2-Cyano-4-methylpyridine (5). This substance was prepared by using the method of Fife.[17] A solution of 4-methylpyridine *N*-oxide (**3**, 1.32 g, 12.1 mmol) in dichloromethane (10 mL) was added to trimethylsilyl cyanide (1.8 mL, 13.6 mmol) at room temperature. Dimethylcarbamyl chloride (1.2 mL, 13.6 mmol) in dichloromethane

Table 2. Photophysical Properties of Blue Phosphorescent Iridium Complexes Ir1−Ir7

	absorption		emission					
complex	MLCT*^{1} (nm)^a	MLCT*^{3} (nm)^a	λ_{em} (nm)^a (298 K)	λ_{em} (nm)^b (298 K)	λ_{em} (nm)^c (77 K)	Stokes shift (cm^{-1})	Φ_p^{d}	τ (μs)
Ir1	366	426	464, 489	462, 489	–	1923	0.22	–
Ir2	370	424	456, 483	456, 483	450, 482	1655	0.39	3.15
Ir3	368	424	456, 484	456, 483	450, 484	1655	0.25	3.57
Ir4	352	422	456, 482	454, 481	–	1768	0.20	–
Ir5	364	416	448, 475	448, 475	444, 475	1717	0.42	3.58
Ir6^e	372	–	459, 489, 521	458, 488	–	–	–	–
Ir7	364	426	469	449, 464	–	2153	0.06	–

^{a}Solution state (2.7×10^{-4} to 1.3×10^{-3} M) in dichloromethane. ^{b}Film state prepared by spin coating dichloromethane solutions with PMMA (5% wt). ^{c}Measured in 2-methyltetrahydrofuran (MTHF) solution. ^{d}In dichloromethane solution using Ir(tpy)$_3$ (Φ_p = 0.45)[10a] as a reference. ^{e}UV−vis absorption and phosphorescence spectra were recorded using nonpurified **Ir6**.

dx.doi.org/10.1021/jo4012514 | J. Org. Chem. 2013, 78, 8054−8064

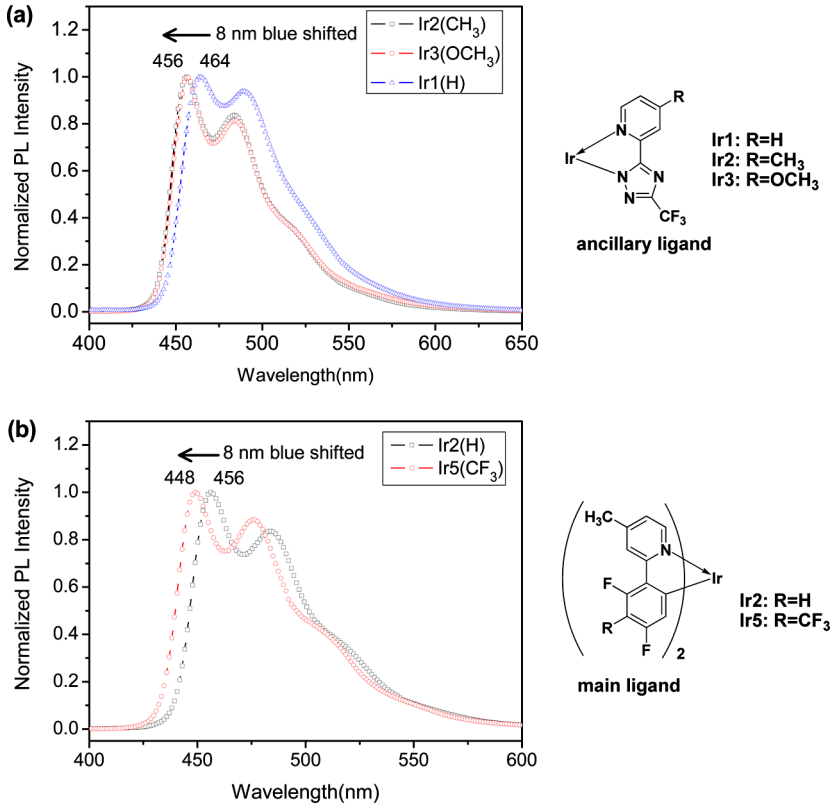

Figure 4. Phosphorescence spectra of **Ir1**–**Ir3** and **Ir5** demonstrating the effects of (a) electron-donating groups at C-4 of the pyridine ring of ancillary ligand and (b) electron-withdrawing groups at C-3 of phenyl ring of main ligand on emission maxima.

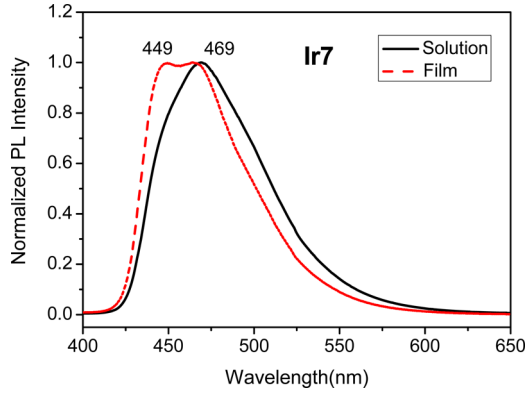

Figure 5. Solution and film state phosphorescence spectra of **Ir7**.

(5.8 mL) was added dropwise to the resulting mixture with stirring. The mixture was stirred at room temperature for 24 h, diluted with 10% aqueous potassium carbonate (20 mL), and stirred for 30 min. The organic layer was separated, and aqueous layer was extracted with dichloromethane. The combined organic layers were dried over anhydrous Na_2SO_4 and concentrated in vacuo, giving a residue that was subjected to column chromatography on silica gel (dichloromethane). The desired 2-cyano-4-methylpyridine (**5**, 1.4 g, 11.6 mmol, 96%) was obtained as a white solid: ^{1}H NMR ($CDCl_3$) δ 8.48 (d, 1H, J = 5.4 Hz), 7.46 (s, 1H), 7.30 (d, 1H, J = 5.4 Hz), 2.37 (s, 3H).

2-Cyano-4-methoxylpyridine (6). A solution of 4-methoxylpyridine *N*-oxide (**4**, 12.8 g, 0.1 mol) in dichloromethane (130 mL) was added to trimethylsilyl cyanide (16.0 mL, 0.1 mmol) at room temperature. Dimethylcarbamyl chloride (11.0 mL, 0.1 mmol) in dichloromethane (20 mL) was then added dropwise to the mixture with stirring. The mixture was stirred at room temperature for 24 h, diluted with 10% aqueous potassium carbonate (100 mL), and stirred for 30 min. The organic layer was separated, and aqueous layer was

Table 3. Frontier Orbital Properties of Blue Phosphorescent Iridium Complexes Ir1–Ir7

complex	HOMO[a]	LUMO[a]	E_g(op-s)[b]	E_g(op-t)[c]
Ir1	−5.59	−2.87	2.97	2.72
Ir2	−5.65	−2.92	3.00	2.73
Ir3	−5.66	−2.93	3.00	2.73
Ir4	−5.65	−2.91	3.02	2.74
Ir5	−5.84	−3.06	3.07	2.78
Ir6[d]	–	–	2.91	–
Ir7	−5.48	−2.76	3.07	2.72

[a]HOMO energies were determined by using the voltage corresponding to the onset point of oxidation and referenced to the Fc/Fc$^+$ couple in CH_2Cl_2 (0.48 eV vs Ag/AgCl). Ferrocene (Fc/Fc$^+$, −4.8 eV). Triplet LUMO energies were calculated using HOMO energies and energy of the triplet-ground state band gap (E_g^{op}). [b]Singlet optical band gaps were calculated from singlet absorption band edge [c]Triplet optical band gaps were calculated from triplet absorption edges. [d]The singlet optical band gap was recorded using unpurified **Ir6**.

extracted with dichloromethane. The combined organic layers were dried over anhydrous Na_2SO_4 and concentrated in vacuo, giving a residue that was subjected to column chromatography on silica gel (ethyl acetate:*n*-hexane = 1:6). The desired 2-cyano-4-methoxylpyridine (**6**, 10.7 g, 80.1 mmol, 80%) was obtained as a white solid:[17] ^{1}H NMR ($CDCl_3$) δ 8.50 (d, 1H, J = 5.4 Hz), 7.21 (d, 1H, J = 2.7 Hz), 6.99 (dd, 1H, J = 5.4 and 2.7 Hz), 3.90 (s, 3H).

Trifluoroacetic acid hydrazide (8). A solution of ethyl trifluoroacetate (**7**, 9.0 mL, 80.0 mmol) in methanol (8.0 mL) was stirred at 0 °C while hydrazine (90.0 mL, 0.1 mol, 1.0 M solution in THF) was added. After 13 h, dichloromethane (100.0 mL) was added to the solution at room temperature, and the solution was then concentrated in vacuo. Dichloromethane (60.0 mL) was added to the residue, and the resulting mixture was stirred at room temperature.

dx.doi.org/10.1021/jo4012514 | J. Org. Chem. 2013, 78, 8054–8064

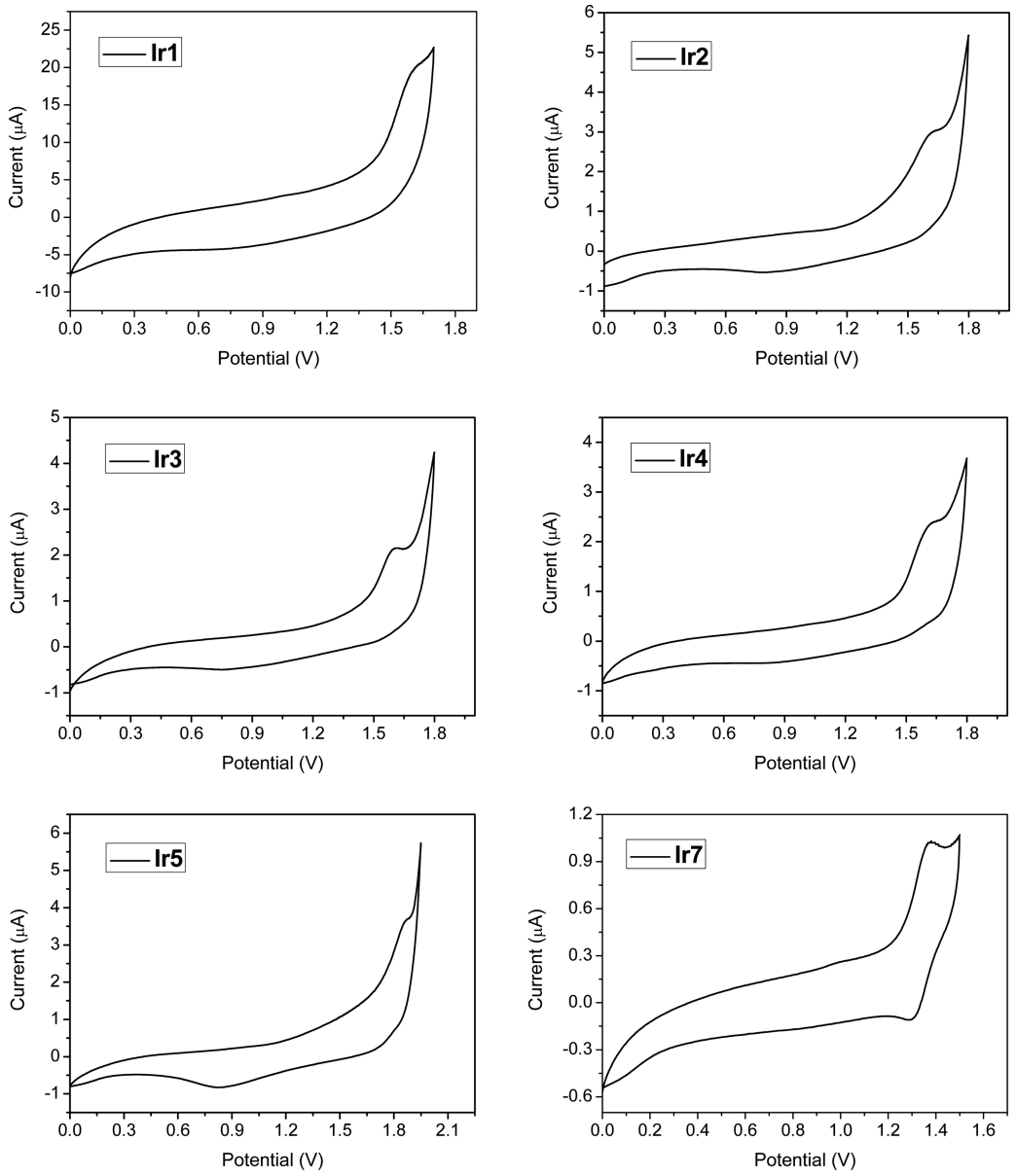

Figure 6. Cyclic voltammograms of **Ir1**–**Ir5** and **Ir7**.

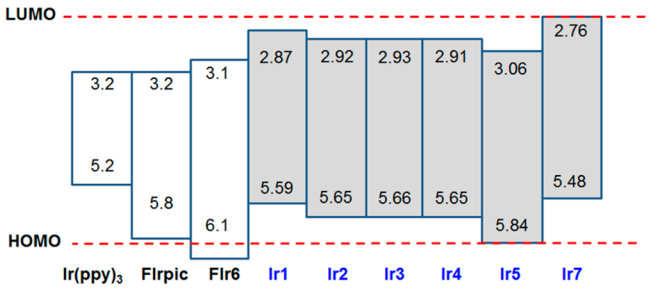

Figure 7. Energy band gap diagram of the synthesized blue phosphorescent complexes **Ir1**–**Ir5** and **Ir7**.

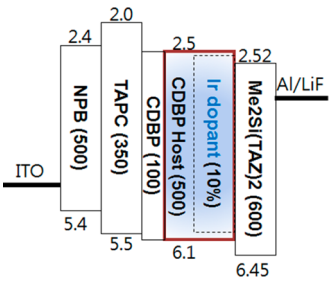

Figure 8. Configuration of the OLED devices using iridium complexes **Ir5** and **Fir6** as dopant materials in the emissive layers (EML).

The formed white solid was removed by filtration, and the filtrate was concentrated in vacuo to yield trifluoroacetic acid hydrazide (**8**, 6.83 g, 53.3 mmol, 67%) as a white gummy liquid:[18] ^{13}C NMR (CD_3OD) δ 158.5 (q, $^2J_{C-F}$ = 36 Hz, $CF_3\underline{C}ONHNH_2$), 118.0 (q, $^1J_{C-F}$ = 283 Hz, $\underline{C}F_3$).

5-(4′-Methylpyridine-2′-yl)-3-trifluoromethyl-1,2,4-triazole (9). A solution of 2-cyano-4-methylpyridine (**5**, 1.3 g, 9.3 mmol) in *N*,*N*-dimethylformamide (60.0 mL) was added to trifluoroacetic acid hydrazide (**8**, 2.2 g, 17.2 mmol), and the resulting mixture was stirred at room temperature for 30 min. A solution of $NaOCH_3$ (28 wt %) in methanol (0.2 g) was added to mixture, which was then stirred at reflux for 2 d. Concentration of the solution in vacuo gave a residue that was dissolved in water. The solution was extracted with ethyl acetate, giving an organic layer that was dried over anhydrous Na_2SO_4 and concentrated in vacuo. The residue was subjected to column

dx.doi.org/10.1021/jo4012514 | J. Org. Chem. 2013, 78, 8054–8064

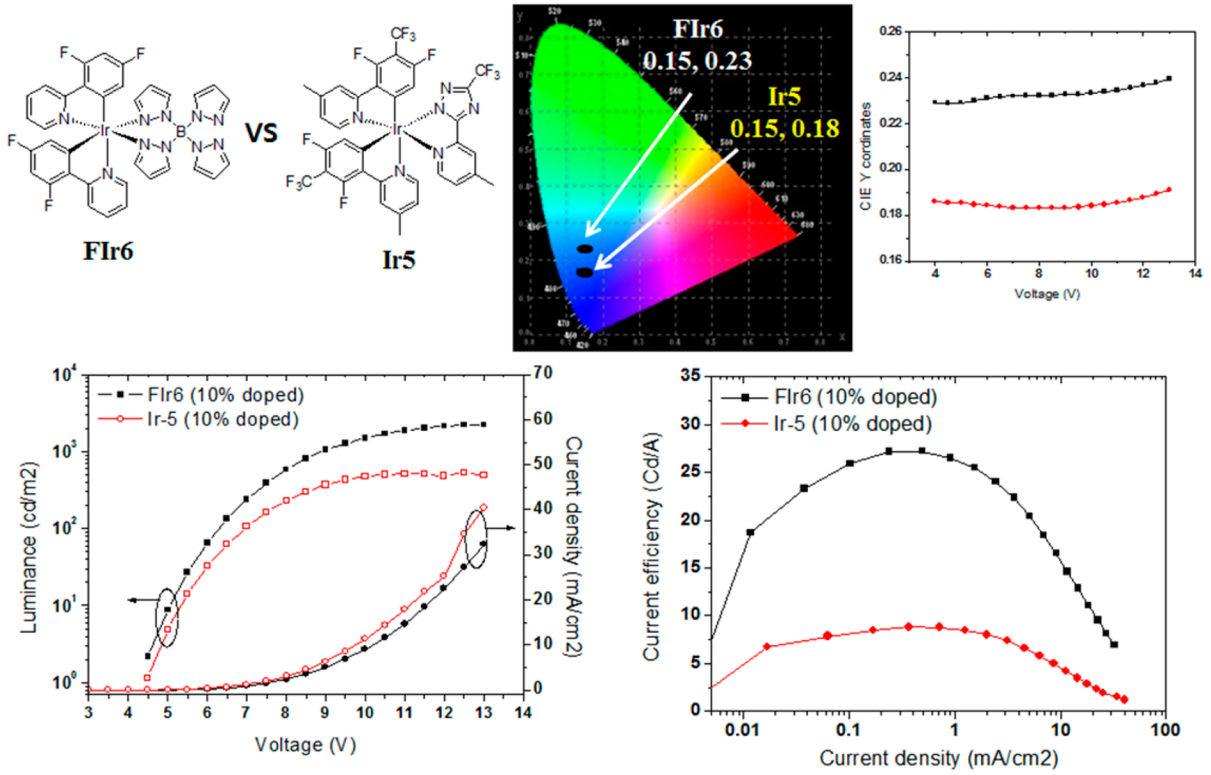

Figure 9. I–V–L curves, luminescence efficiencies, and CIE coordinates of devices constructed using **Ir5** and **Fir6**.

chromatography on silica gel (ethyl acetate:chloroform = 1:5) to give **9** (0.6 g, 2.5 mmol, 27%) as a white solid: ^{1}H NMR ($CDCl_3$) δ 8.70 (d, 1H, J = 5.4 Hz), 8.21 (s, 1H), 7.36 (d, 1H, J = 5.4 Hz), 2.51 (s, 3H); ^{13}C NMR ($CDCl_3$) δ 155.4, 155.1 (q, $^2J_{C-F}$ = 39 Hz, C-CF_3), 150.6, 149.1, 144.5, 126.9, 123.6, 119.2 (q, $^1J_{C-F}$ = 268 Hz, CF_3), 21.1; HRMS (FAB) $[M + H]^+$, Calcd for $C_9H_8F_3N_4$ 229.0701, found 229.0703.

5-(4′-Methoxypyridine-2′-yl)-3-trifluoromethyl-1,2,4-triazole (10). A solution of 2-cyano-4-methoxypyridine (**6**, 2.0 g, 15.0 mmol) in *N*,*N*-dimethylformamide (50.0 mL) was added to **8** (2.5 g, 19.5 mmol), and the resulting solution was stirred at room temperature for 30 min. A solution of $NaOCH_3$ (28 wt %) in methanol (1.4 g) was added, and the mixture was stirred at reflux for 3 d and concentrated in vacuo. The residue was dissolved in water. The aqueous solution was extracted with ethyl acetate. The organic layer was dried over anhydrous Na_2SO_4 and concentrated in vacuo, giving a residue that was subjected to column chromatography on silica gel (ethyl acetate:chloroform = 1:5) to give **10** (0.7 g, 3.0 mmol, 20%) as a colorless liquid: ^{1}H NMR ($CDCl_3$) δ 8.18 (d, 1H, J = 6.3 Hz), 7.32 (s, 1H), 6.78 (d, 1H, J = 6.3 Hz), 4.24 (s, 3H); ^{13}C NMR ($CDCl_3$) δ 170.0, 152.0 (q, $^2J_{C-F}$ = 39 Hz, C-CF_3), 151.894, 146.7, 143.2, 118.8 (q, $^1J_{C-F}$ = 268 Hz, CF_3), 114.7, 113.8, 39.1; HRMS (FAB) $[M]^+$, Calcd for $C_9H_7F_3N_4O$, 244.0572, found 244.0570.

5-(Pyridine-2′-yl)-3-trifluoromethyl-1,2,4-triazole (12). A solution of 2-cyanopyridine (**11**, 0.93 mL, 9.6 mmol) in ethanol (30.0 mL) was added to **8** (2.5 g, 19.5 mmol). The resulting mixture was stirred at room temperature for 30 min and then diluted with a solution of $NaOCH_3$ (28 wt %) in methanol (1.4 g). The resulting solution was stirred at reflux for 2 h and concentrated in vacuo. The residue was heated at 130 °C for 12 h and dissolved in water. The aqueous solution was extracted with chloroform. The organic layer was dried over anhydrous Na_2SO_4 and concentrated in vacuo, giving a residue that was subjected to column chromatography on silica gel (ethyl acetate:chloroform = 1:5) to give **12** (1.06 g, 5.0 mmol, 52%) as a yellow solid:[12] ^{1}H NMR ($CDCl_3$) δ 8.84 (d, 1H, J = 5.1 Hz), 8.35 (d, 1H, J = 8.1 Hz), 7.98 (ddd, 1H, J = 8.1 Hz, 8.1 Hz, 1.5 Hz), 7.54 (ddd, 1H, J = 8.1 Hz, 5.1 Hz, 1.2 Hz).

2-(2′,4′-Difluorophenyl)-4-picoline (16). In a 100 mL one-neck round bottomed flask equipped with a condenser were placed 2,4-difluorophenyl boronic acid (**13**, 1.1 g, 7.0 mmol), 2-bromo-4-picoline (**14**, 1.2 g, 7.0 mmol), $Ba(OH)_2{\cdot}8H_2O$ (6.2 g, 19.5 mmol), and $Pd(PPh_3)_4$ (0.2 g, 0.3 mmol). The flask was evacuated and filled with N_2 gas. 1,4-Dioxane (20.0 mL) and H_2O (7.0 mL) were added. The mixture was stirred at reflux for 30 h under a N_2 atmosphere and cooled to room temperature. Concentration in vacuo gave a residue that was poured into a dichloromethane. The formed precipitate was removed by filtration, and the filtrate was washed with 1 M NaOH (30 mL × 2) and saturated aqueous NaCl (30 mL). The organic layer was dried over anhydrous Na_2SO_4 and concentrated in vacuo, giving a residue that was subjected to column chromatography on silica gel (ethyl acetate:hexane = 1:6) to give 2-(2′,4′-difluorophenyl)-4-picoline (**16**, 1.0 g, 4.9 mmol, 70%) as a colorless oil:[9] ^{1}H NMR ($CDCl_3$) δ 8.54 (d, 1H, J = 5.1 Hz), 7.90–7.98 (m, 1H), 7.54 (s, 1H), 7.06 (d, 1H, J = 5.1 Hz), 6.94–7.00 (m, 1H), 6.85–6.92 (m, 1H), 2.41 (s, 3H).

2-(2′4′-Difluorophenyl)-4-(dimethylamino)pyridine (17). In a 100 mL one-neck round-bottom flask equipped with a condenser were placed 2,4-difluorophenyl boronic acid (**13**, 1.1 g, 6.9 mmol), 2-bromo-4-(dimethylamino)pyridine (**15**, 1.2 g, 6.9 mmol), $Ba(OH)_2{\cdot}8H_2O$ (6.5 g, 20.6 mmol), $Pd(PPh_3)_4$ (0.4 g, 0.3 mmol), and 1,4-dioxane/H_2O (1/3, 34.3 mL). The flask was evacuated and filled with N_2 gas. The mixture was stirred at reflux for 30 h under a N_2 atmosphere and cooled to room temperature. Concentration in vacuo gave a residue that was poured into a dichloromethane (30 mL). The formed precipitate was removed by filtration, and the filtrate was washed with satd. NaCl (aq) (30 mL), dried over anhydrous sodium sulfate, and concentrated in vacuo, giving a residue that was subjected to column chromatography on silica gel (ethyl acetate:hexane = 1:2) to provide 2-(2′,4′-difluorophenyl)-4-(dimethylamino)pyridine (**17**, 1.2 g, 5.0 mmol, 72%) as a yellow oil:[19] ^{1}H NMR ($CDCl_3$) δ 8.30 (d, 1H, J = 5.7 Hz), 7.87–7.95 (m, 1H), 6.87–6.99 (m, 3H), 6.48 (d, 1H, J = 5.7 Hz), 3.03 (s, 6H).

2-(2′,4′-Difluoro-3′-iodophenyl)-4-picoline (18). A 2.0 M solution (12.5 mL, 25.0 mmol) of lithium diisopropylamide in heptane/THF/ethylbenzene was added dropwise to a THF (43.0 mL) solution of **16** (3.5 g, 10.6 mmol) at −78 °C. The resulting solution was stirred for 1 h. Iodine (6.1 g, 24 mmol) dissolved in THF (35 mL) was added

dx.doi.org/10.1021/jo4012514 | J. Org. Chem. 2013, 78, 8054–8064

to the solution, and the mixture was stirred for 3 h at −78 °C, warmed to room temperature, and diluted with water (300 mL). The solution was extracted with diethyl ether, giving an organic layer that was washed with water (100 mL), satd. $Na_2S_2O_3$ (aq) (100 mL) and satd. NaCl (aq) (100 mL), dried over anhydrous Na_2SO_4, and concentrated in vacuo. The residue was subjected to column chromatography on silica gel (eluent = ethyl acetate:hexane = 1:6) to give 2-(2′,4′-difluoro-3′-iodophenyl)-4-picoline (**18**, 5.4 g, 16.3 mmol, 65%) as a white solid:[9] ^{1}H NMR ($CDCl_3$) δ 8.55 (d, 1H, J = 5.1 Hz), 7.90−7.98 (m, 1H), 7.55 (s, 1H), 7.10 (d, 1H, J = 5.1 Hz), 6.98−7.03 (m, 1H), 2.41 (s, 3H).

2-[2′,4′-Difluoro-3′-(trifluoromethyl)phenyl]-4-picoline (19). A mixture of copper(I) iodide (1.7 g, 9.1 mmol) and spray-dried anhydrous potassium fluoride (0.5 g, 9.1 mmol) was heated with a heat gun under reduced pressure while being gently shaken until the color changed to greenish yellow.[20] After the addition of **18** (2.0 g, 6.0 mmol), the vessel was Ar-purged, and *N*-methylpyrrolidinone (10 mL) and (trifluoromethyl)trimethylsilane (1.8 mL, 12.1 mmol) were added. The suspension was vigorously stirred for 24 h at room temperature and poured into 28% aqueous ammonia (66 mL). The solution was extracted with dichloromethane. The organic layer was washed with water and brine, dried over anhydrous sodium sulfate, and concentrated in vacuo, giving a residue that was subjected to column chromatography on silica gel (ethyl acetate:hexane = 1:6) yielding 2-[2′,4′-difluoro-3′-(trifluoromethyl)phenyl]-4-picoline (**19**, 0.8 g, 3.1 mmol, 53%) as a colorless oil:[9] ^{1}H NMR ($CDCl_3$) δ 8.52 (d, 1H, J = 5.1 Hz), 8.08−8.16 (m, 1H), 7.53 (s, 1H), 7.03−7.09 (m, 2H), 2.37 (s, 3H).

Synthesis of Iridium(III)-μ-Chlorobridged Dimer Complexes 20−22. *Typical Procedure.* A mixture of iridium(III) chloride trihydrate (83.0 mg, 0.2 mmol), 2-(2′4′-difluorophenyl)-4-picoline (**16**, 0.12 g, 0.6 mmol) in 2-ethoxyethanol/water (4 mL; 3/1) was stirred at reflux under a nitrogen atmosphere for 18 h. After cooling to room temperature, the mixture was concentrated in vacuo, giving a residue that was dissolved in water. The mixture was extracted with dichloromethane, and the organic layer was washed with water and brine, dried over sodium sulfate, and concentrated in vacuo to give the iridium(III)-μ-chlorobridged dimer complex **20**. Complexes **21** and **22** were prepared from the corresponding 2-phenylpyridine ligand **17** and **19**, respectively, by using a similar procedure.

20 (74%): ^{1}H NMR ($CDCl_3$) δ 8.91 (d, 4H, J = 5.7 Hz), 8.10 (s, 4H), 6.59 (d, 4H, J = 5.7 Hz), 6.30 (m, 4H), 5.31 (dd, 4H, J = 10.5 Hz, 2.7 Hz), 2.66 (s, 12H).

21 (70%): ^{1}H NMR ($CDCl_3$) δ 8.87 (d, 4H, J = 5.7 Hz), 8.21 (s, 4H), 6.70 (d, 4H, J = 5.7 Hz), 5.40 (d, 4H, J = 10.5 Hz), 2.72 (s, 12H).

22 (54%):[19] ^{1}H NMR ($CDCl_3$) δ 9.21 (d, 1H, J = 5.7 Hz), 8.86 (d, 1H, J = 5.7 Hz), 7.37 (m, 2H), 6.70−7.00 (m, 4H), 5.83 (dd, 1H, J = 5.7 Hz, 2.0 Hz), 5.35 (dd, 1H, J = 5.7 Hz, 2.0 Hz), 3.19 (s, 6H), 3.16 (s, 6H).

Synthesis of Iridium(III) Complexes Ir1−Ir7. *Typical Procedure.* A mixture of dimer complex **20** (0.13 g, 0.11 mmol), ancillary ligand **9** (0.06 g, 0.26 mmol), and sodium carbonate (160 mg) in 2-ethoxyethanol (7 mL) was heated at 135 °C for 24 h under a nitrogen atmosphere. After cooling to room temperature, the solution was concentrated in vacuo, and water was added to the residue. The mixture was extracted with dichloromethane. The organic layer was dried over anhydrous sodium sulfate and concentrated in vacuo, giving a residue that was subjected to column chromatography on silica gel (dichloromethane:hexane = 1:10). The solid obtained was recrystallized from dichloromethane/hexane to give **Ir2** (0.04g, 0.05 mmol, 45%) as a green yellow solid. Iridium(III) complexes **Ir1** and **Ir3−Ir7** were prepared from the corresponding ancillary ligands **12**, **9**, and **10**, respectively, by using a similar procedure.

Ir1 (38%): ^{1}H NMR ($CDCl_3$) δ 8.29 (d, 1H, J = 5.4 Hz), 8.06 (s, 1H), 8.04 (s, 1H), 7.57−7.73 (m, 1H) 7.56 (d, 1H, J = 5.4 Hz), 6.81 (d, 1H, J = 4.8 Hz), 6.72 (d, 1H, J = 4.8 Hz), 6.55−6.40 (m, 2H), 5.79 (dd, 1H, J = 8.4 Hz, 2.4 Hz), 5.69 (dd, 1H, J = 8.4 Hz, 2.4 Hz), 2.51 (s, 6H); HRMS (FAB) $[M]^+$, Calcd for $C_{32}H_{20}F_7N_6Ir$ 814.1267, found 814.1270.

Ir2 (45%): ^{1}H NMR ($CDCl_3$) δ 8.12 (s, 1H), 8.07 (s, 1H), 8.03 (s, 1H) 7.55 (d, 1H, J = 5.4 Hz), 7.53 (d, 1H, J = 5.4 Hz), 7.25 (d, 1H, J = 5.4 Hz), 7.00 (d, 1H, J = 5.4 Hz), 6.79 (d, 1H, J = 5.4 Hz), 6.70 (d, 1H, J = 5.4 Hz), 6.52−6.36 (m, 2H), 5.78 (dd, 1H, J = 8.4 Hz, 2.4 Hz), 5.70 (dd, 1H, J = 8.4 Hz, 2.4 Hz), 2.48 (s, 3H), 2.47 (s, 3H); HRMS (FAB) $[M]^+$, Calcd for $C_{33}H_{22}F_7N_6Ir$ 828.1423, found 828.1437.

Ir3 (48%): ^{1}H NMR ($CDCl_3$) δ 8.04 (s, 1H), 8.00 (s, 1H), 7.72 (d, 1H, J = 2.4 Hz), 7.52 (d, 1H, J = 6.0 Hz), 7.45 (d, 1H, J = 6.0 Hz), 7.23 (d, 1H, J = 6.0 Hz), 6.77 (d, 1H, J = 6 Hz), 6.70 (d, 1H, J = 6 Hz), 6.69 (d, 1H, J = 6 Hz), 6.49−6.33 (m, 2H), 5.75 (dd, 1H, J = 8.4 Hz, 2.7 Hz), 5.68 (dd, 1H, J = 8.4 Hz, 2.7 Hz), 3.92 (s, 3H), 2.46 (s, 6H); HRMS (FAB) $[M]^+$, Calcd for $C_{33}H_{22}OF_7N_6Ir$ 844.1373, found 844.1390.

Ir4 (30%):[9] ^{1}H NMR ($CDCl_3$) δ 8.88 (d, 1H, J = 5.4 Hz), 8.63 (s, 1H), 8.58 (s, 1H), 8.01−7.96 (m, 1H), 7.91−7.82 (m, 1H), 7.60 (d, 1H, J = 5.4 Hz), 6.66 (d, 1H, J = 4.8 Hz), 6.62 (d, 1H, J = 4.8 Hz), 5.75−5.62 (m, 2H), 2.47 (s, 6H).

Ir5 (51%): ^{1}H NMR ($CDCl_3$) δ 8.14 (s, 2H), 8.10 (s, 1H), 7.53 (d, 2H, J = 5.7 Hz), 7.28 (d, 1H, J = 5.7 Hz), 7.08 (d, 1H, J = 5.7 Hz), 6.90 (d, 1H, J = 5.7 Hz), 6.82 (d, 1H, J = 5.7 Hz), 5.89 (d, 1H, J = 10.5 Hz), 5.79 (d, 1H, J = 10.5 Hz), 2.52 (s, 6H), 2.49 (s, 3H); HRMS (FAB) $[M + H]^+$, Calcd for $C_{35}H_{21}F_{13}N_6Ir$ 965.1249, found 965.1245.

Ir7 (49%): ^{1}H NMR ($CDCl_3$) δ 8.08 (s, 1H), 7.58 (d, 1H, J = 5.7 Hz), 7.44 (s, 1H), 7.38 (s, 1H), 7.21 (d, 1H, J = 6.9 Hz), 6.96 (d, 1H, J = 5.7 Hz), 6.92 (d, 1H, J = 6.9 Hz), 6.47−6.32 (m, 2H), 6.16 (dd, 1H, J = 6.9 Hz, 2.7 Hz), 6.08 (dd, 1H, J = 6.9 Hz, 2.7 Hz), 5.91 (dd, 1H, J = 8.5 Hz, 2.7 Hz), 5.86 (dd, 1H, J = 8.5 Hz, 2.7 Hz), 3.06 (s, 6H), 3.05 (s, 6H), 2.43 (s, 3H); HRMS (FAB) $[M]^+$, Calcd for $C_{35}H_{28}F_7N_8Ir$ 886.1954, found 886.1960.

Optical Measurements. The absorption and photoluminescence (PL) spectra were measured using a spectrometer and a fluorescence spectrometer, respectively, in chloroform at room temperature. Phosphorescence spectra were obtained using absorption wavelengths for their MLCT^1* as excitation wavelengths in dichloromethane, and phosphorescence quantum yields (Φ_p) were estimated using a dichloromethane solution of $Ir(tpy)_3$ as a standard with a known value of Φ_p = 0.45[10a] at room temperature.

Triplet Lifetime Measurements. The phosphorescence spectra at 77 K were measured by an intensified charge-coupled device detector equipped with a monochromator. The samples were excited using the 355 nm pulses of the third harmonic generation from a Q-switched nanosecond Nd:YAG laser (pulse width of 4.5 ns fwhm). Temporal profiles were measured by a monochromator equipped with a photomultiplier and a digital oscilloscope.

Electrochemistry. Electrochemical measurements of iridium complexes **Ir1−Ir7** were made by using cyclic voltammetry (CV). Cyclic voltammograms were recorded on CHI600C in dichloromethane (HPLC grade) solution with three electrodes consisting of a Pt disc working electrode (2 mm diameter), a Pt wire counter electrode, and a Ag/AgCl reference electrode at room temperature. Tetrabutylammonium perchlorate and Cp_2Fe/Cp_2Fe^+ redox couple were used as a supporting electrolyte and a secondary internal reference (−4.8 eV), respectively.

Crystallography. All X-ray crystallographic data were collected on an automatic diffractometer with a graphite-monochromated Mo Kα radiation (λ = 0.71073 Å) and a CCD detector at ambient temperature. Thirty six frames of two-dimensional diffraction images were collected and processed to obtain the cell parameters and orientation matrix. The data were corrected for Lorentz and polarization effects. Absorption effects were corrected by using the empirical method. The structures were solved by employing direct methods (SHELXS 97) and refined by using full-matrix least-squares techniques (SHELXL 97). The non-hydrogen atoms were refined anisotropically, and hydrogen atoms were placed in calculated positions and refined using a riding model.

■ ASSOCIATED CONTENT

Ⓢ Supporting Information

^{1}H and ^{13}C NMR spectra of all previously unidentified compounds, Phosphorescence decay spectra and detailed crystallographic data in CIF format of crystals **Ir2**, **Ir3**, and

dx.doi.org/10.1021/jo4012514 | J. Org. Chem. 2013, 78, 8054−8064

Ir5. This material is available free of charge via the Internet at http://pubs.acs.org.

AUTHOR INFORMATION

Corresponding Author

*E-mail: ucyoon@pusan.ac.kr.

Notes

The authors declare no competing financial interest.

ACKNOWLEDGMENTS

This work was supported by National Research Foundation of Korea Grant funded by the Korean Government (2012R1A1A2007158 for U. C. Yoon).

REFERENCES

(1) Baldo, M. A.; O'Brien, D. F.; Thompson, M. E.; Forrest, S. R. *Phys. Rev. B* **1999**, *60*, 14422.
(2) Baldo, M. A.; Thompson, M. E.; Forrest, S. R. *Pure Appl. Chem.* **1999**, *71*, 2095.
(3) (a) Brooks, J.; Babayan, Y.; Lamansky, S.; Djurovich, P. I.; Tsyba, I.; Bau, R.; Thompson, M. E. *Inorg. Chem.* **2002**, *41*, 3055. (b) Laskar, I. R.; Hsu, S. F.; Chen, T. M. *Polyhedron* **2005**, *24*, 881.
(4) (a) Adachi, C.; Baldo, M. A.; Forrest, S. R.; Thompson, M. E. *Appl. Phys. Lett.* **2000**, *77*, 904. (b) Brooks, J.; Babayan, Y.; Lamansky, S.; Djurovich, P.; Tsyba, I.; Bau, R.; Thompson, M. E. *Inorg. Chem.* **2002**, *41*, 3055.
(5) (a) Tokito, S.; Iijima, T.; Suzuri, Y.; Kita, H.; Tsuzuki, T.; Sato, F. *Appl. Phys. Lett.* **2003**, *83*, 569. (b) Holmes, R. J.; D'Andrade, B. W.; Forrest, S. R.; Ren, X.; Li, J.; Thompson, M. E. *Appl. Phys. Lett.* **2003**, *83*, 3818.
(6) (a) Turro, N. J. *Modern Molecular Photochemistry*; The Benjamin/Cummings Publishing Co., Inc.; Menlo Park, CA, 1978. (b) Murov, S. L.; Carmichael, I.; Hug, G. L. *Handbook of Photochemistry*; Marcel Dekker: New York, 1993.
(7) Baldo, M. A.; Thompson, M. E.; Forrest, S. R. *Nature* **2000**, *403*, 750.
(8) Hay, P. J. *J. Phys. Chem. A* **2002**, *106*, 1634.
(9) Takizawa, S.; Echizen, H.; Nishida, J.; Tsuzuki, T.; Tokito, S.; Yamashita, Y. *Chem. Lett.* **2006**, *35*, 748.
(10) (a) Grushin, V. V.; Herron, N.; LeCloux, D. D.; Marshall, W. J.; Petrov, V. A.; Wang, Y. *Chem. Commun.* **2001**, 1494. (b) Tamayo, A. B.; Alleyne, B. D.; Djurovich, P.; Lamansky, S.; Tsyba, I.; Ho, N. N.; Bau, R.; Thompson, M. E. *J. Am. Chem. Soc.* **2003**, *125*, 12971. (c) Coppo, P.; Plummer, E. A.; Cola, L. D. *Chem. Commun.* **2004**, 1774.
(11) Sammakia, T.; Hurley, T. B. *J. Org. Chem.* **1999**, *64*, 4652.
(12) Hagiwara, K.; Aihara, T.; Tanigawa, H.; Sano, S.; Shimoda, S.; Sano, H. Pyridyltriazole Compounds, Processes for Producing The Same and Agricultural and Horticultural Germicides, PCT Int. Appl. WO99/002518, Jan 21, 1999.
(13) Lamansky, S.; Djurovich, P.; Murphy, D.; Abdel-Razaq, F.; Kwong, R.; Tsyba, I.; Bortz, Mui, M. B.; Bau, R.; Thompson, M. E. *Inorg. Chem.* **2001**, *40*, 1704.
(14) Li, J.; Djurovich, P. I.; Alleyne, B. D.; Yousufuddin, M.; Ho, N. N.; Thomas, J. C.; Peters, J. C.; Bau, R.; Thompson, M. E. *Inorg. Chem.* **2005**, *44*, 1713.
(15) Taylor, E. C.; Crovetti, A. *Organic Syntheses*; Rabjohn, N., Ed.; John Wiley & Sons: New York, 1963; Collect. Vol. *IV*, pp 655–656.
(16) Shuman, R. T.; Ornstein, P. L.; Paschal, J. W.; Gesellchen, P. D. *J. Org. Chem.* **1990**, *55*, 738.
(17) Fife, W. K. *J. Org. Chem.* **1983**, *48*, 1375.
(18) Sitzmann, M. E. *J. Fluorine Chem.* **1995**, *70*, 31.
(19) Jin, S. H.; Jung, O. S.; Kim, Y. I.; Hyun, M. H.; Lee, J. W.; Yoon, U. C.; Nazeeruddin, M. K.; Klein, C.; Graetzel, M. PCT Int. Appl. (2007), WO 2007042474.
(20) Cottet, F.; Schlosser, M. *Eur. J. Org. Chem.* **2002**, 327.